^{70,72}Ge$(n,p)^{70,72}$Ga reactions: Suppression of Gamow-Teller strength near $N=40$

M. C. Vetterli,[1] K. P. Jackson,[1] A. Celler,[2] J. Engel,[3] D. Frekers,[1] O. Häusser,[1,4] R. Helmer,[1] R. Henderson,[1] K. H. Hicks,[1,*] R. G. Jeppesen,[4,†] B. Larson,[4] B. Pointon,[4,‡] A. Trudel,[4] and S. Yen[1]

[1]*TRIUMF, 4004 Wesbrook Mall, Vancouver, British Columbia, Canada V6T 2A3;*
[2]*University of Western Ontario, London, Ontario, Canada N6A 3K7; and*
[3]*Bartol Research Institute, University of Delaware, Newark, Delaware 19716*
[4]*Simon Fraser University, Burnaby, British Columbia, Canada V5A 1S6*

(Received 18 September 1991)

The ^{70,72}Ge$(n,p)^{70,72}$Ga reactions have been measured at a beam energy of 200 MeV in order to study the behavior of Gamow-Teller (GT) strength near the $N=40$ subshell closure. The GT quenching factor extracted for ^{70}Ge is consistent with results for ^{54}Fe and with calculations done on the quasiparticle random-phase-approximation model if they are renormalized by a factor of about 0.6. The quasiparticle random-phase approximation predicts a drastic reduction in concentrated GT strength from ^{70}Ge to ^{72}Ge which is also seen in the data. These results are relevant to models of supernovae.

PACS number(s): 25.40.Fq, 24.30.Cz, 27.50.+e

I. INTRODUCTION

Charge-exchange reactions at intermediate energy have been very useful in the study of spin-isospin excitations of the nucleus [1,2,3]. In particular, the dominance of the isovector spin-flip component, $V_{\sigma\tau}$, of the nucleon-nucleon interaction at energies above ≈ 100 MeV acts as a filter for Gamow-Teller (GT) transitions at low momentum transfer. The isobaric analog resonance (IAR) which dominates the (p,n) spectrum at low energy is suppressed in intermediate-energy (p,n) reactions. This property of nucleon charge-exchange reactions makes it possible to study GT strength relatively free of background at intermediate energies. Furthermore, the IAR is not excited in (n,p) reactions because of isospin selection rules. Background due to the presence of the IAR is therefore not a problem in the (n,p) direction.

This paper describes a study of the suppression of GT strength near the subshell closure at $N=40$ using the (n,p) reaction on ^{70}Ge and ^{72}Ge. These data, which are related to electron-capture rates, are relevant to models which describe supernova formation.

Electron-capture rates in fp shell nuclei are important input parameters to models of stellar collapse leading to the formation of a supernova [4,5]. At the end of the burning cycle of a star, there is no more nuclear fusion to oppose gravitational collapse. However, there are a large number of free electrons present and the relativistic electron gas pressure stabilizes the star. Stellar collapse is initiated when the mass of the core exceeds the Chandrasekhar mass $M_{\rm Ch}=5.8\langle Y_e^2\rangle M_\odot$, where Y_e is the ratio of the number of electrons to the number of baryons and $M_\odot$ is the mass of the sun. When the collapsing core reaches nuclear density, nucleon-nucleon repulsion causes it to bounce back and create a shock wave which propagates outward. This could lead to an explosion, ejecting material from the envelope and leaving behind a neutron star or a black hole. Detailed discussion of stellar collapse can be found in Refs. [6,7].

Current models have trouble producing a supernova because the shock wave loses too much energy as it propagates through the envelope. These models are sensitive to the mass of the collapsing core and therefore to Y_e. The latter, in turn, is sensitive to electron-capture rates since this process will reduce the number of free electrons present while leaving the baryon number unchanged. Because the star is at the end of its cycle, the core is made up mainly of fp shell nuclei, notably in the Fe region. Studies of electron-capture rates in some of these nuclei (^{48}Ti, ^{51}V, ^{54}Fe, ^{56}Fe, ^{58}Ni, and ^{59}Co) have been done at TRIUMF [8–11] using the nucleon charge-exchange facility described below. Gamow-Teller transitions ($\Delta T=\Delta S=1$, $\Delta L=0$) are the prime determinant of the electron-capture rate. Of particular interest is what happens to the GT strength as the neutron shell fills. This filling is brought on in a collapsing star by electron capture itself which changes protons to neutrons in the nucleus. In the simple shell model, as the neutron shell fills, the number of final states available for electron capture is reduced until the transitions are blocked to first order. This would increase the value of Y_e and hence the mass of the collapsing core. We choose the germanium iso-

*Present address: Ohio University, Athens, OH 45701.
†Present address: Los Alamos Natl. Laboratory (P-3), Los Alamos, NM 87545.
‡Present address: BCIT, Vancouver, BC, Canada.

topes to study the effects of the filling of the neutron shell since they are the closest stable nuclei.

The data are compared to quasiparticle random-phase-approximation (RPA) calculations which have been used to explain the suppression of double β decay [12].

II. STRUCTURE OF ^{70}Ge AND ^{72}Ge

In the simple spherical shell model, ^{70}Ge has four protons in the $p_{3/2}$ shell [$\pi(p_{3/2})^4$], and six neutrons in the $f_{5/2}$ shell [$\nu(f_{5/2})^6$]. The $p_{1/2}$ neutron shell is empty and the $\pi(p_{3/2})\rightarrow\nu(p_{1/2})$ GT transition is allowed. In ^{72}Ge, the $p_{1/2}$ neutron shell is filled and the GT transition is blocked. Hence, we expect to see GT strength in ^{70}Ge(n,p) but none in ^{72}Ge(n,p). This picture is certainly much too naive. The $\pi(f_{7/2})\rightarrow\nu(f_{5/2})$ GT channel is opened by two-particle–two-hole excitations out of the $\nu(f_{5/2})$ shell. More complicated excitations would open even more channels.

The situation is in reality much more complex than described above. The germanium isotopes are not spherical but deformed. In fact, there is evidence of a shape transition from oblate to prolate between $N=40$ and 42. Vergnes *et al.* [13] found that the sharp maximum in the cross section to 0^+ excited states observed in both (p,t) and (t,p) reactions occurs for final nuclei which differ by two neutrons. This is similar to the situation in $N=88-90$ nuclei where there is a shape transition and excited 0^+ states are shape isomers. However, Vergnes *et al.* find that there is a larger overlap between the $N=40$ and 42 ground states than in the heavier nuclei. Furthermore, studies of (p,t) reactions at sub-Coulomb triton energies [14] indicate that the anomalous shape of the 0^+ angular distributions can be explained without recourse to a shape transition.

The picture that emerges from all this work is that the germanium isotopes are quite soft but that the shape transition, if it exists, is not as pronounced as in $N=88-90$ nuclei. The ground and excited states of ^{70,72}Ge and ^{70,72}Ga are likely to be complicated configurations which include the $p_{3/2}$, $f_{5/2}$, $p_{1/2}$, and $g_{9/2}$ orbitals. In fact, Ardouin *et al.* [15] have found that a $\pi(f_{5/2})^2(p_{3/2})^2$ component of up to 72% in the ^{72}Ge ground-state (g.s.) wave function is consistent with their data. Given the uncertainty on the structure, a RPA calculation which spans a large model space does not seem inappropriate. We will compare our results to such a calculation.

III. EXPERIMENTAL METHOD

A. TRIUMF CHARGEX Facility

The TRIUMF nucleon charge-exchange (CHARGEX) facility is discussed in detail elsewhere [16]. A short description is included here for completeness. The setup for (n,p) experiments is shown schematically in Fig. 1.

A proton beam from the TRIUMF cyclotron strikes a neutron production target located 92 cm upstream of the pivot of the medium resolution spectrometer [17] (MRS) on beam line 4B. A compact sweeping magnet bends the proton beam 20° to the right into a shielded beam dump. The neutrons from the primary target continue undeflected by the magnetic field and strike the secondary target of interest at the MRS pivot. The ^{7}Li$(p,n)^7$Be reaction is used to produce a nearly monoenergetic beam of neutrons. This reaction populates the ground state and the unresolved 429-keV state in ^{7}Be; this contributes to the energy spread of the neutron beam. Furthermore, a long continuum tail is produced which amounts to about 1% of the peak area per MeV. A method of obtaining the neutron line shape for deconvolution from the (n,p) spectra is described in Ref. [8]. The neutron flux at the (n,p) targets is about 10^5/(sec/cm^2) for a beam intensity of 350 nA and a 110-mg/cm^2-thick ^{7}Li target.

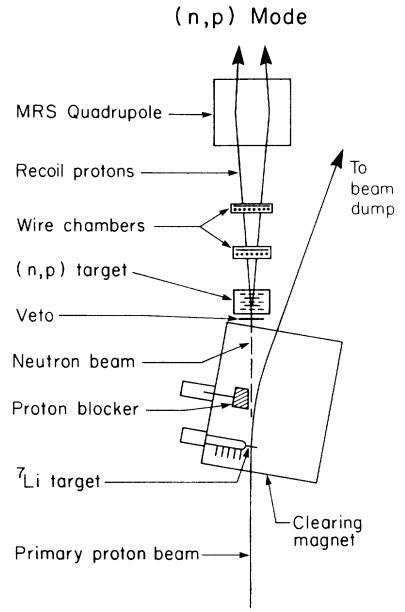

FIG. 1. TRIUMF charge-exchange facility in the (n,p) mode. The neutron beam is produced by the ^{7}Li$(p,n)^7$Be reaction and the protons from the secondary (n,p) scattering are detected in the MRS. The primary proton beam is deflected 20° into a shielded beam dump.

The (n,p) target box consists of six target layers separated by proportional wire chambers [18]. A thin scintillator upstream of the target box vetoes charged particles. The first wire chamber consists of a double plane, both of which also act as vetos. The target arrangement for this experiment was Be (142 mg/cm^2), 2 ^{72}Ge (173.1 mg/cm^2, 181.0 mg/cm^2), 2 ^{70}Ge (205.4 mg/cm^2, 198.7 mg/cm^2), CH_2 (44.3 mg/cm^2). Two other stacks were used, one with six CH_2 targets, the other with all positions empty except the last one (CH_2) used for normalization. The pattern of hit wires in the target box determines in which of the six layers the (n,p) reaction took place. Corrections are made for energy loss in the subsequent targets and relatively good resolution ($\approx$1 MeV) can be recovered. Furthermore, the layered arrangement allows the use of a target of known cross section (usually CH_2) in one of the positions to normalize the data independent of beam current, dead time, and MRS

efficiency. A good efficiency is required for the target wire planes to reduce the occurrence of target misidentification. A method for determining these inefficiences can be found in Refs. [8,18]. Two front-end chambers (FEC's) at the entrance to the MRS are used to raytrace back to the (n,p) target. Software gates on the target coordinates are used to eliminate background from scattered beam particles or neutrons undergoing reactions outside the target.

The proton beam was integrated using the beam dump as a Faraday cup. A small reverse leakage current was monitored and remained relatively constant throughout the experiment ($I_R \approx -2.5$ to -4.0 nA compared to $I_{\text{beam}} \approx 350-450$ nA).

B. Germanium targets

Germanium oxide targets were not used because the Q values of the various (n,p) reactions [$Q(^{16}\text{O}) = -9.64$ MeV, $Q(^{70}\text{Ge}) = -0.88$ MeV, $Q(^{72}\text{Ge}) = -3.21$ MeV] are such that we would get only 6.5–8.5 MeV in excitation energy free of background from the $^{16}\text{O}(n,p)^{16}\text{N}$ reaction. Isotopically enriched germanium (98.45% for ^{70}Ge, 97.86% for ^{72}Ge) was obtained on loan from Oak Ridge National Laboratory. Both isotopes were in powder form. The targets were mounted in aluminum frames (2 cm×5 cm×0.159 cm) with 25.4-μm-thick (4.7 mg/cm^2) beryllium windows. Beryllium was chosen because of the low $^9\text{Be}(n,p)^9\text{Li}$ cross section. A thick Be target was included at the front of the stack and the yield was scaled to the thickness of the windows and subtracted from the Ge data.

IV. RESULTS

Data were taken at five MRS central angles (0°, 3°, 6°, 10°, and 15°) for a proton beam energy of 200 MeV. These angles correspond to average scattering angles in the laboratory frame of 1.8°, 2.8°, 5.8°, 9.8°, and 14.8°. The differences arise from the solid angle subtended by the secondary (n,p) targets with respect to the neutron production target and the acceptance of the MRS.

Corrections were made for the difference in neutron flux and MRS solid angle for each individual target layer using the $(CH_2)^6$ stack. Corrections were also made for the acceptance of the spectrometer as a function of excitation energy determined by sweeping the peak from the $^1\text{H}(n,p)$ across the focal plane by varying the magnetic field. This measurement also fixed the momentum calibration of the spectrometer.

One of the major concerns with the secondary target box is the problem of target misidentification. This happens mostly when a proton from one target is identified as coming from the target immediately downstream of it due to an inefficiency in the wire plane separating them (target leak through). This effect is corrected by subtracting from the downstream spectrum a fraction of the upstream spectrum determined from the measured inefficiencies of the target wire planes [8]. Because of this effect, targets with large yields, such as CH_2, are placed in the last position of the stack.

Since the targets are interspersed with wire chambers, a small contribution to the spectra arises from the detector gas and windows which is corrected by the subtraction of spectra recorded without the (n,p) targets. This contribution is very small except at $Q = 0$ MeV where the $\text{H}(n,p)$ reaction has a peak, and only significant for ^{70}Ge (Q value of -0.88 MeV). The presence of the Be windows, a small correction, was also taken into account as described above. Tight cuts were necessary on both horizontal and vertical target coordinates to eliminate contributions from the target frames.

The $^7\text{Li}(p,n)^7\text{Be}$ reaction does not produce strictly monoenergetic neutrons and the tail of the distribution must be deconvoluted from the data. This procedure is described in Ref. [8].

The results for the cross section versus the excitation energy in gallium are shown in Figs. 2 and 3. The relatively weak peaks at $E_x \approx 0.5$ and 4.5 MeV in ^{70}Ga are consistent with $L = 0$ angular distributions and are identified below as GT transitions. There is no obvious GT peak in the $^{72}\text{Ge}(n,p)$ spectrum. Note that the small peak at negative excitation energy is a remnant of the $\text{H}(n,p)$ reaction in the wire chamber gas and windows. The broad bumps at $E_x \approx 10-15$ MeV in both nuclei have angular distributions which agree with an $L = 1$ shape

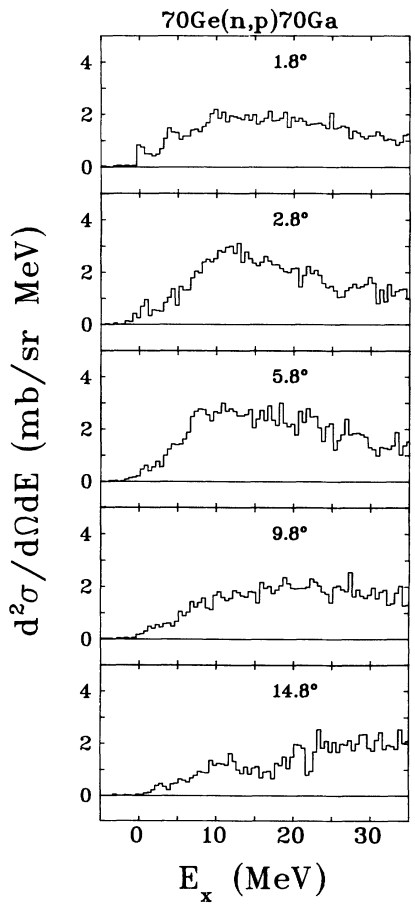

FIG. 2. $^{70}\text{Ge}(n,p)^{70}\text{Ga}$ cross section at five angles between 1.8° and 14.8°. The small peaks at 0.5 and 4.5 MeV in the 1.8° spectrum are identified as Gamow-Teller transitions.

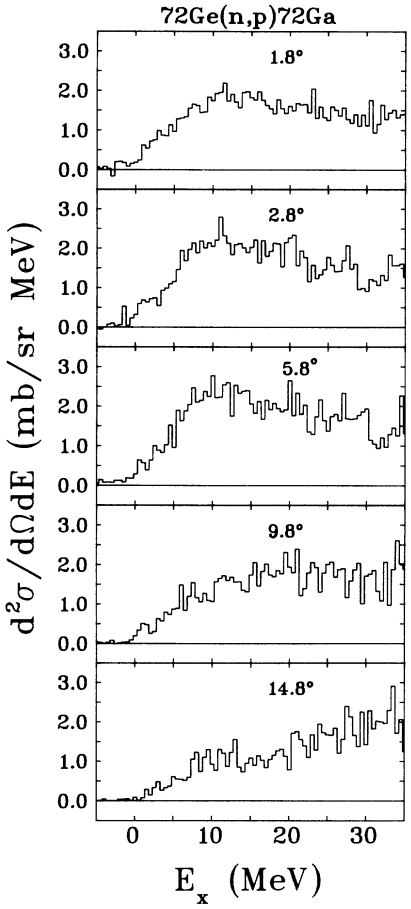

FIG. 3. ^{72}Ge(n,p)^{72}Ga cross section at five angles between 1.8° and 14.8°. There are no obvious peaks in the 1.8° data as predicted by the QRPA model. The small peak at 1.8° and negative E_x is a remnant of the H(n,p) reaction.

characteristic of a dipole resonance. Ge(n,p) cross sections were obtained relative to those of the H(n,p) reaction observed with the CH_2 target at the back of the stack. A value of 53.2 mb/sr was used for the ^{1}H(n,p) cross section in the laboratory frame at 1.8°. This was taken from a phase-shift analysis of N-N data [19].

V. DISCUSSION

A. Multipole decomposition

To extract strengths for the different giant resonances, in particular, the Gamow-Teller strength, a multipole decomposition of the cross sections was done. The data were summed into 1-MeV bins and angular distributions were generated for each one. Theoretical angular distributions for each angular momentum transfer were calculated using the distorted-wave impulse approximation (program DW81 [20]) with the Franey-Love interaction [21] at 200 MeV. The optical potentials for the distortions in DW81 were generated using the program MAINX8 [22] and a three-parameter Fermi distribution with parameters $W=0$, $R=4.409$, $Z=0.583$ taken from electron scattering on ^{70}Zn [23]. The following simple shell-model configurations were assumed for the final states of the ^{70}Ge(n,p) reaction (initial state $\pi[(f_{7/2})^8(p_{3/2})^4]\nu[(f_{7/2})^8(p_{3/2})^4(f_{5/2})^6]$ with respect to a ^{40}Ca core):

$$\Delta L=0: \ [\pi(p_{3/2})^3,\nu(p_{1/2})]_{1^+},$$

$$\Delta L=1: \ [\pi(f_{7/2})^7,\nu(g_{9/2}]_{1^-},$$

$$\Delta L=2: \ [\pi(p_{3/2})^3,\nu(p_{1/2})]_{2^+}.$$

The same shapes for the angular distribution were used for ^{72}Ge. The variation in the $\Delta L=2$ angular distributions for the different J^π_{final} is small and the choice of the configuration is not crucial in this case. However, the shapes for $\Delta L=1$ ($J^\pi=0^-,1^-,2^-$) vary somewhat depending on J^π_{final}. Without a detailed shell-model calculation, it is difficult to known how to combine the three shapes. The simplest procedure is to choose one. The multipole decomposition is very sensitive to the $\Delta L=1$ shape, especially at small angles. Celler *et al.* [24] have shown that the distorted-wave impulse approximation (DWIA) does not reproduce the experimental $\Delta L=1$ angular distribution for ^{15}N(n,p)^{15}C. They also show that the small, extracted GT strength disappears if the experimental shapes are used for $\Delta L=1$. This effect will induce systematic errors in the determination of GT strength, particularly since this strength is weak in our case.

It should be noted that the fitting procedure will lump

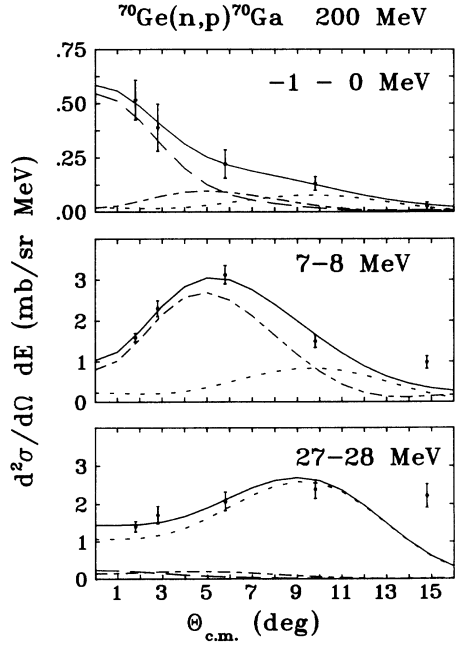

FIG. 4. Typical angular distributions for the ^{70}Ge(n,p)^{70}Ga reaction. The panels are labeled by excitation energy. The distributions are dominated from top to bottom by $\Delta L=0,1,2$, respectively. The dashed curve is the $\Delta L=0$ fraction of the cross section while the dash-dotted and dotted curves correspond to $\Delta L=1$ and 2, respectively. The full curve is the total fit to the data.

all $\Delta L \geq 2$ strength into the $\Delta L = 2$ shape. The Q-value dependence of the theoretical angular distributions is taken into account by doing the calculations from $E_x = 0$ to 40 MeV in 10-MeV steps and interpolating in between. The angular distribution for each energy bin was fitted independently with a computer program which uses the MINUIT minimization routines. This procedure is described in Refs. [8,25]. Typical angular distributions are shown in Fig. 4. The three plots are for excitation energy bins where each of the three shapes ($\Delta L = 0,1,2$) dominates.

The results for the decomposition of the ^{70}Ge data at 1.8° and 5.8° are plotted in Figs. 5 and 6, respectively. The "right-hatched" region (hatched from the bottom left to upper right) shows the $\Delta L = 2$ strength, while the "left-hatched" region (hatched from the bottom right to the upper left) represents the $\Delta L = 1$ strength. The $\Delta L = 0$ strength is shown as the crosshatched region. It is clear that the two peaks at about 0.5 and 4.5 MeV at 1.8° are predominantly $\Delta L = 0$. The multipole decomposition does not extract reliably small components of the cross section. Because of this, we only consider GT strength where the $\Delta L = 0$ component dominates. This also corresponds to the region where GT strength is predicted by theory. The cross section integrated below 8 MeV is 8.72±0.24 mb/sr. Note that the uncertainty does not include any error on the H(n,p) cross section taken from the phase-shift analysis. The multipole decomposition indicates that 41% of this is $\Delta L = 0$. An uncertainty of 15% in this fraction (i.e., ±6.2%) is estimated based on experience with the decomposition program (e.g., by varying the shapes of the theoretical angular distributions). We obtain

$$^{70}\text{Ge}: \ \sigma_{L=0}(1.8°) = 3.6 \pm 0.55 \text{ mb/sr} .$$

The results for ^{72}Ge at 1.8° and 5.8° are shown in Figs. 7 and 8, respectively. The meaning of the hatching is the same as in the previous plots. The decomposition yields a broad distribution with no clear peaks. Integrating over the region where GT strength is predicted ($E_x \leq 10$ MeV), and using the fact that the decomposition gives a 34% $\Delta L = 0$ fraction below 10 MeV, we get

$$^{72}\text{Ge}: \ \sigma_{L=0}(1.8°) = 3.7 \pm 0.6 \text{ mb/sr} ,$$

where we have again included an arbitrary uncertainty of 15% on the $\Delta L = 0$ fraction. In this case, this is certainly an underestimate of the error because of the lack of a strong GT peak.

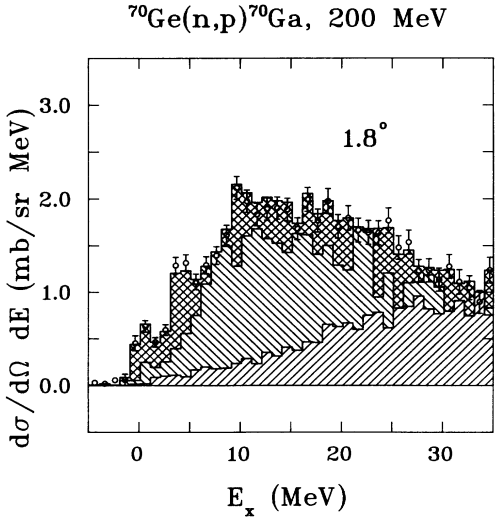

FIG. 5. Multipole decomposition of the ^{70}Ge$(n,p)^{70}$Ga cross section at 1.8°. The crosshatched region is the $\Delta L = 0$ component while the left- and right-hatched regions are $\Delta L = 1$ and 2, respectively.

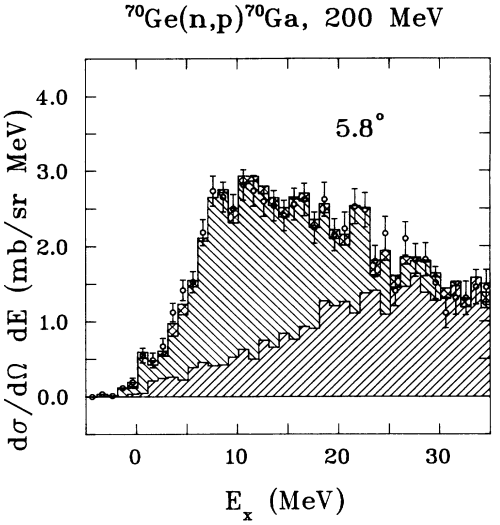

FIG. 6. Multipole decomposition of the ^{70}Ge$(n,p)^{70}$Ga cross section at 5.8°. The hatching is the same as in Fig. 5.

B. Alternative method

As mentioned above, the uncertainty in the $\Delta L = 1$ shape can cause spurious GT strength to appear in the

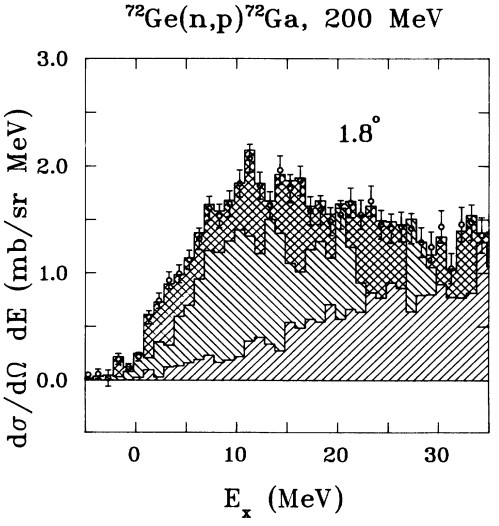

FIG. 7. Multipole decomposition of the ^{72}Ge$(n,p)^{72}$Ga cross section at 1.8°. The hatching is the same as in Fig. 5.

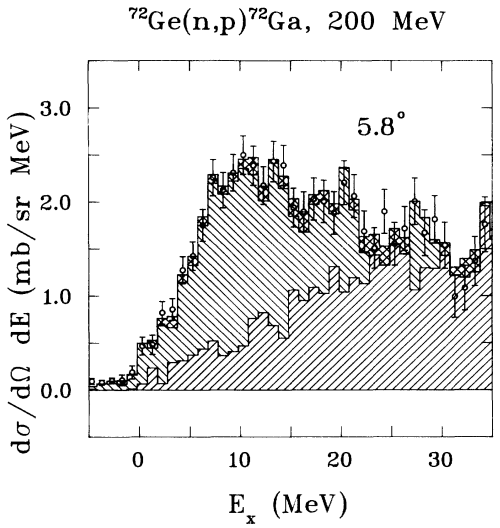

FIG. 8. Multipole decomposition of the ^{72}Ge(n,p)^{72}Ga cross section at 5.8°. The hatching is the same as in Fig. 5.

multipole decomposition, especially when this strength is weak. We have attempted to determine the magnitude of the error by using an independent method to extract the $\Delta L=0$ cross section. This simple method has been used by Rapport *et al.* [26]. It is based on the fact that the $\Delta L=0$ cross section drops dramatically between 0° and 6° while the $\Delta L=1$ cross section varies much less. The 6° data are used to approximate the $\Delta L=1$ contribution to the 0° spectrum at low excitation energy. In practice, the 6° data are normalized to the 0° data at $E_x \approx 10$ MeV, and then subtracted from the latter. What is left is taken to be the $\Delta L=0$ cross section. This procedure is illustrated in Figs. 9 and 10 for ^{70}Ge and ^{72}Ge. If we include an arbitrary uncertainty in this procedure of 20%, we obtain, for $E_x \leq 8$ MeV,

$$\sigma_{L=0}(1.8°, {}^{70}\text{Ge}) = 3.1 \pm 0.6 \text{ mb/sr} ,$$

$$\sigma_{L=0}(1.8°, {}^{72}\text{Ge}) = 1.0 \pm 0.3 \text{ mb/sr} .$$

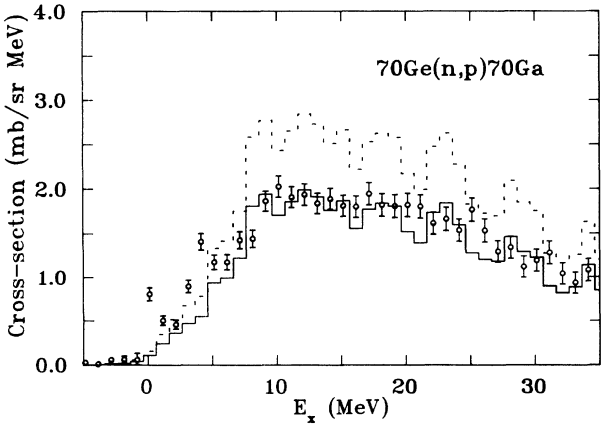

FIG. 9. Illustration of the determination of the $\Delta L=0$ component of the ^{70}Ge(n,p)^{70}Ga cross section at 1.8° using the 5.8° data to approximate the $\Delta L=1$ component. The data points are for the 1.8° cross section. The dashed curve is the raw 5.8° data which are subtracted from the 1.8° after being normalized to the latter at $E_x \approx 10$ MeV (full curve).

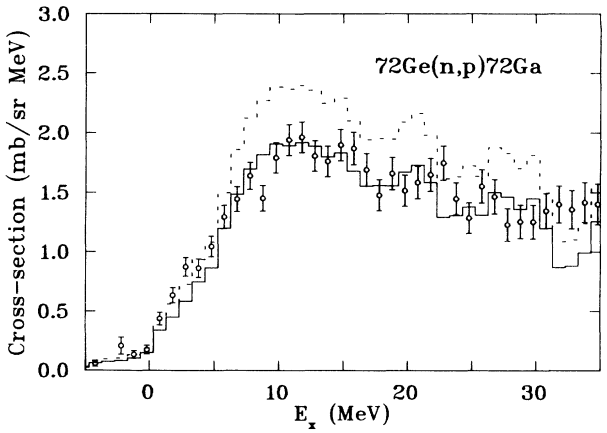

FIG. 10. Same as Fig. 9 but for the ^{72}Ge(n,p)^{72}Ga reaction.

We point out that caution must be exercised in the interpretation of these results. In particular, this procedure implies that GT strength which has the same distribution in excitation energy as the spin-dipole resonance is missed.

C. Gamow-Teller strength

The charge-exchange cross sections at 200 MeV have been calibrated against known β decays [27,28]. In this mass region, the ratio σ/B (GT) is about [28] 5. However, since this number is for $q=\omega=0$, where q is the momentum transfer and ω the energy transfer, we must extrapolate our data to 0°. This was done with the DWIA and the ratio $\sigma(0°)/\sigma(1.8°)$ was found to be 1.16. Therefore, for ^{70}Ge with the multipole decomposition:

$$\sigma_{\text{GT}}(0°) = 4.2 \pm 0.6 \rightarrow B(\text{GT}) = 0.84 \pm 0.13 ,$$

$$E_x \leq 8.1 \text{ MeV} ,$$

for ^{70}Ge with method 2:

$$\sigma_{\text{GT}}(0°) = 3.6 \pm 0.7 \rightarrow B(\text{GT}) = 0.72 \pm 0.14 ,$$

$$E_x \leq 7.6 \text{ MeV} ,$$

for ^{72}Ge with the multipole decomposition:

$$\sigma_{\text{GT}}(0°) = 4.3 \pm 0.7 \rightarrow B(\text{GT}) = 0.86 \pm 0.14 ,$$

$$E_x \leq 9.8 \text{ MeV} ,$$

for ^{72}Ge with method 2:

$$\sigma_{\text{GT}}(0°) = 1.2 \pm 0.2 \rightarrow B(\text{GT}) = 0.23 \pm 0.05 ,$$

$$E_x \leq 7.8 \text{ MeV} .$$

The results for ^{70}Ge are similar and agree within the uncertainties. We can probably consider them as an upper and lower limit on the GT strength. On the other hand, the numbers for ^{72}Ge do not agree. Due to the problems associated with both methods of extracting the $\Delta L=0$ component of the cross section, we can only quote an upper limit on the GT strength in ^{72}Ge (≤ 0.86), which is very uncertain.

D. Quasiparticle random-phase-approximation calculations

We now compare our results for the Gamow-Teller strength to predictions of the quasiparticle random-phase-approximation model (QRPA) of Vogel, Zirnbauer, and Engel [12]. This is the same model that gives good agreement with the ^{54}Fe$(n,p)^{54}$Mn and ^{54}Fe$(p,n)^{54}$Co data [8] if the calculations are renormalized by a factor of between 0.62 and 0.68. The results of the QRPA calculation for the (n,p) reaction on ^{70}Ge and ^{72}Ge are plotted in Fig. 11 where they are compared to the $\Delta L=0$ component of the cross section deduced from the multipole decomposition. The location of the GT strength in ^{70}Ge is predicted rather well although the relative strength of the peaks is not correctly predicted.

The integrated GT strength for ^{70}Ge$(n,p)^{70}$Ga is $B(\mathrm{GT})=1.33$. This gives a quenching factor of between 0.54 and 0.63 for ^{70}Ge depending on which method is used to extract the $\Delta L=0$ component. The predicted GT strength for ^{72}Ge$(n,p)^{72}$Ga is $B(\mathrm{GT})=0.3$. Due to the uncertainty in B(GT) for ^{72}Ge, no quenching factor can be reliably determined for this nucleus.

The quenching factor for ^{70}Ge is consistent with the ^{54}Fe results. Furthermore, the QRPA predicts very little strength for ^{72}Ge which is consistent with our observations. The QRPA model reasonably predicts GT strength in the fp shell within a quenching factor of about 0.6–0.7, although the reduction of strength for ^{72}Ge agrees only qualitatively with the data.

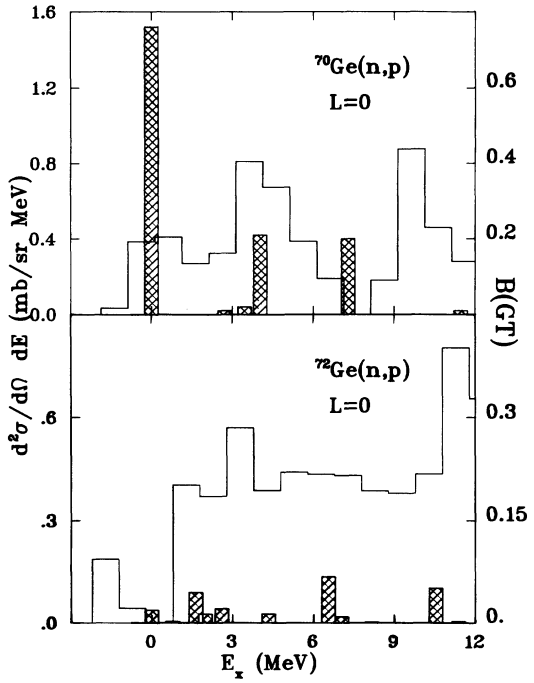

FIG. 11. Comparison of the $\Delta L=0$ cross section for the ^{70}Ge(n,p) and ^{72}Ge(n,p) reactions determined by the multipole decomposition of the 1.8° data with the predictions of the QRPA model. Recall that the strength at negative E_x, in particular for ^{72}Ge, is left over from the subtraction of the H(n,p) yield determined from the empty runs.

E. Spin-dipole strength

For completeness we give the integrated $\Delta L=1$ cross section at 5.8° which is identified as the spin-dipole resonance:

$$\sigma(^{70}\mathrm{Ge},\Delta L=1,\theta=5.8°)=29.8\pm5\ \mathrm{mb/sr}\ ,$$
$$E_x\leq 25.1\ \mathrm{MeV}\ ,$$
$$\sigma(^{72}\mathrm{Ge},\Delta L=1,\theta=5.8°)=23.4\pm4\ \mathrm{mb/sr}\ ,$$
$$E_x\leq 25.3\ \mathrm{MeV}\ ,$$

where we have included an estimated 15% uncertainty on the multipole decomposition.

VI. CONCLUSIONS

The ^{70,72}Ge$(n,p)^{70,72}$Ga reactions have been measured at 200 MeV to study the distribution of Gamow-Teller strength in nuclei near the $N=40$ subshell closure. These data are relevant to models of supernovae since the electron-capture rates in nuclei in this region of the periodic table influence the value of Y_e, the ratio of free electrons to baryons in the star.

The distribution of GT strength for the ^{70}Ge$(n,p)^{70}$Ga reaction is reasonably well reproduced by the quasiparticle random-phase-approximation model of Vogel *et al.* while the summed strength is smaller by a factor of between 0.54 and 0.63. These results are consistent with (n,p) and (p,n) data on ^{54}Fe. The extraction of GT strength from the ^{72}Ge$(n,p)^{72}$Ga is made more difficult than for ^{70}Ge by the absence of concentrated $\Delta L=0$ strength. The conclusions drawn from these data are therefore of a qualitative nature only. The QRPA does not predict any concentrated GT strength which is consistent with the data.

In conclusion, we have observed a reduction in the Gamow-Teller strength in germanium isotopes when the neutron number is increased from 38 to 40. This is consistent with a QRPA model which correctly predicts total GT strength for fp shell nuclei, within a quenching factor of about 0.6–0.7, although the behavior for ^{72}Ge agrees only qualitatively with the data.

[1] C. D. Goodman, C. A. Goulding, M. B. Greenfield, J. Rapaport, D. E. Bainum, C. C. Foster, W. G. Love, and F. Petrovich, Phys. Rev. Lett. **44**, 1755 (1980).
[2] C. Gaarde, Nucl. Phys. **A396**, 127c (1983).
[3] K. P. Jackson and A. Celler, in *Spin Observables of Nuclear Probes*, edited by C. J. Horowitz, C. D. Goodman, and G. E. Walker (Plenum, New York, 1988), p. 139.
[4] G. M. Fuller, Astrophys. J. **252**, 741 (1982).
[5] J. Cooperstein and J. Wambach, Nucl. Phys. **A420**, 591 (1984).
[6] G. E. Brown, H. A. Bethe, and G. Baym, Nucl. Phys. **A375**, 481 (1982).
[7] H. A. Bethe and G. Brown, Sci. Am. **252**, 60 (1985).
[8] M. C. Vetterli *et al.*, Phys. Rev. C **40**, 559 (1989).

[9] K. P. Jackson *et al.*, TRIUMF Experiment E384.
[10] W. P. Alford *et al.*, Nucl. Phys. **A514**, 49 (1990).
[11] W. P. Alford *et al.*, TRIUMF Experiment E629.
[12] J. Engel, P. Vogel, and M. R. Zirnbauer, Phys. Rev. C **37**, 731 (1988).
[13] M. N. Vergnes, G. Rotbard, F. Guilbault, D. Ardouin, C. Lebrun, E. R. Flynn, D. L. Hanson, and S. D. Orbesen, Phys. Lett. **72B**, 447 (1978).
[14] A. Becker, E. A. Bakkum, and R. Kamermans, Phys. Lett. **110B**, 199 (1982).
[15] D. Ardouin, R. Tamisier, M. Vergnes, G. Rotbard, J. Kalifa, G. Berrier, and B. Grammaticos, Phys. Rev. C **12**, 1745 (1975).
[16] R. Helmer, Can. J. Phys. **65**, 588 (1987).
[17] MRS manual, TRIUMF, unpublished.
[18] R. S. Henderson, W. P. Alford, D. Frekers, O. Häusser, R. L. Helmer, K. H. Hicks, K. P. Jackson, C. A. Miller, M. C. Vetterli, and S. Yen, Nucl. Instrum. Methods A **257**, 97 (1987).
[19] R. A. Arndt and L. D. Soper, Scattering Analysis Interactive Dial-in (SAID) Program, 1984, unpublished.
[20] J. R. Comfort, computer code DW81, Arizona State University.
[21] M. A. Franey and W. G. Love, Phys. Rev. C **31**, 488 (1985).
[22] Computer code MAINX8, modifications by R. G. Jeppesen, unpublished.
[23] C. W. de Jager, H. De Vries, and C. de Vries, At. Data Nucl. Data Tables **14**, 479 (1974).
[24] A. Celler *et al.*, Phys. Rev. C **43**, 639 (1991).
[25] M. A. Moinester, Can. J. Phys. **65**, 660 (1987).
[26] J. Rapaport, T. Taddeucci, T. P. Welch, C. Gaarde, J. Larsen, D. J. Horen, E. Sugarbaker, P. Koncz, C. C. Foster, C. D. Goodman, C. A. Goulding, and T. Masterson, Nucl. Phys. **A410**, 371 (1983); C. D. Goodman and S. D. Bloom, unpublished.
[27] K. P. Jackson *et al.*, Phys. Lett. B **201**, 25 (1988).
[28] T. N. Taddeucci, C. A. Goulding, T. A. Carey, R. C. Byrd, C. D. Goodman, C. Gaarde, J. Larsen, D. Horen, J. Rapaport, and E. Sugarbaker, Nucl. Phys. **A469**, 125 (1987).